Soft Matter

View Online
Dynamic Article Links

Cite this: DOI: 10.1039/c0sm01007c

www.softmatter.org

PAPER

Shape- and size-dependent patterns in self-oscillating polymer gels†‡

Irene Chou Chen,[a] Olga Kuksenok,[b] Victor V. Yashin,[b] Ryan M. Moslin,[c] Anna C. Balazs[b] and Krystyn J. Van Vliet[d]

Received 16th September 2010, Accepted 30th November 2010
DOI: 10.1039/c0sm01007c

Polymeric hydrogels that exhibit autonomous, coupled chemical and mechanical oscillations are a unique example of synthetic, active soft matter. Here, we explore the effects of gel aspect ratio and absolute dimensions on pattern formation in hydrogels undergoing the Belousov-Zhabotinsky (BZ) reaction. We synthesize and analyze N-isopropylacrylamide gels containing covalently bound BZ catalyst and polyacrylamide-silica gel composites containing physically associated BZ catalyst. Through both experiments and computational simulations, we demonstrate that the oscillating chemical patterns within BZ gels can be altered by changing the shape and size of the gel, and that these patterns evolve over long timescales. In our simulations, we utilize an improved Oregonator model, which explicitly accounts for the total concentration of the catalyst grafted onto the polymer network. We find that the three-dimensional simulations of the BZ gels successfully reproduce patterns, oscillation periodicity, and catalyst concentration-dependence observed in experiments. Together, these findings validate our theoretical and computational approaches for modeling chemomechanical coupling in active, chemo-responsive gels, and enable future studies that exploit the shape- and size-confinement effects of self-oscillating reactions.

Introduction

An impressive range of functional polymers has been demonstrated to change in color, hydrophobicity, conductivity, stiffness, or physical dimensions in response to external stimuli.[1–4] In particular, active hydrogels and gel composites that exhibit appreciable and reversible swelling in response to cues such as temperature, pH, and electromagnetic field have been engineered as environmental sensors,[5] actuators capable of mechanical work,[6] and materials of dynamically tunable stiffness for biological cell scaffolds.[7] Typically, such active soft matter requires a perturbation in external conditions to induce or reverse these property changes. In contrast, Yoshida *et al.* and Konotop *et al.* have synthesized gels capable of undergoing autonomous, periodic changes in both volume and color in the absence of continuous external perturbation.[8–10] The spontaneous nature of these chemomechanical oscillations is reminiscent of biological processes such as cardiac rhythms. However, the origin of this synthetic functionality is the Belousov-Zhabotinsky (BZ) reaction, a complex but well-established self-oscillating chemical reaction that is characterized by oxidation of an organic acid substrate in the presence of a strong acid and a transition-metal catalyst.[11]

The pattern formation of the BZ reaction can be monitored visually due to color variations indicative of the catalyst oxidation state.[11] Yoshida *et al.*'s studies of the BZ gel, N-isopropylacrylamide-*co*-ruthenium(II)tris(2,2′-bipyridine) (NIPAAm-*co*-Ru(bpy)$_3$), showed that narrow strips exhibited sub-mm scale waves of color that traversed down the length of the (1 × 1 × 20 mm) gel over minute timescales. In contrast, much smaller cubes (0.5 mm edges) exhibited homogeneous, synchronized color change and swelling.[12] Balazs *et al.* developed a computational approach to model such oscillations.[13–15] These simulations predicted a number of fascinating effects[16,17] including oscillations triggered by applied mechanical force,[18,19] and strain-controlled synchronization of oscillations in heterogeneous gels.[20] However, to date, these systematic predictions of responsive chemomechanics in BZ gels have not yet been validated experimentally. Here, we pair new experiments and simulations to validate our theoretical and computational approaches to modeling chemomechanical coupling in such active gels, and to consider whether changes in BZ gel size and aspect ratio can alter pattern formation and oscillation characteristics. We chose our simulation parameters to match experimental conditions. Importantly, we also modify the reaction kinetics employed in

[a]*Department of Chemical Engineering, Massachusetts Institute of Technology, Cambridge, MA, 02139, USA*
[b]*Department of Chemical Engineering, University of Pittsburgh, Pittsburgh, PA, 15261, USA*
[c]*Department of Chemistry, Massachusetts Institute of Technology, Cambridge, MA, 02139, USA*
[d]*Department of Materials Science and Engineering, Massachusetts Institute of Technology, Cambridge, MA, 02139, USA*

† This paper is part of a *Soft Matter* themed issue on Active Soft Matter. Guest editors: Fred MacKintosh and Mike Cates.

‡ Electronic supplementary information (ESI) available: further experimental details and movies. See DOI: 10.1039/c0sm01007c

our original simulation approach[13,21,15] by incorporating an improved Oregonator model that explicitly accounts for the total concentration of the BZ catalyst in the governing equations.[22] (The previous model was formulated in terms of the volume fraction of catalyst in the oxidized state, rather than the total volume fraction of catalyst.) This modified approach allows us to model for the first time the effects of the total concentration of catalyst on the dynamics of three-dimensional BZ gel samples. By doing so, we demonstrate that the results of our computational simulations are in agreement with our experimental findings.

Results and discussion

First, we demonstrate that significant confinement of the BZ reaction within a gel can alter the resulting chemical wave patterns. The BZ wave patterns in single-phase solutions have been well studied, and spiral and target waves are the major modes of pattern formation.[23,24] Fig. 1A shows that these chemical waves can be of high visual contrast when ferroin is used as the catalyst; the ferroin color alternates between red (reduced) and blue (oxidized). Figs. 1B–C. show the same BZ reaction, but now confined within two small pieces of polyacrylamide hydrogel that differ in shape and size. To obtain Figs. 1B–C, we synthesized the polyacrylamide-silica gel composite containing electrostatically bound ferroin as described by Konotop *et al.*[10] Then, the gel was cut into a disc of 8 mm diameter (Fig. 1B) and a square of 3.6 mm width (Fig. 1C). The images in Figs. 1B–C were obtained at early reaction times, directly after immersion of the catalyst-containing gels in a solution of necessary BZ reactants. Figs. 1B–C demonstrate that the nature of BZ pattern formation in gels depends on the gel size and shape. Namely, the larger gel disc in Fig. 1B exhibits spiral waves similar to those observed in solution (Fig. 1A), whereas in the smaller, square gel (Fig. 1C), waves originate at the corners and propagate inward. Due to the small size of this square gel, such waves eliminate each other near the gel center before they can be classified as a spiral or target wave. Here, it is the global geometry-driven nature of the wave fronts that becomes apparent for gels of sufficiently small size. We note that the similarity in pattern formation between BZ solutions and cm-scale BZ polymers was reported previously for various gels and resins undergoing the BZ reaction.[25] However, Fig. 1 shows that modification of BZ gel size and shape can give rise to oscillation patterns that are visually distinct from those observed in solutions.

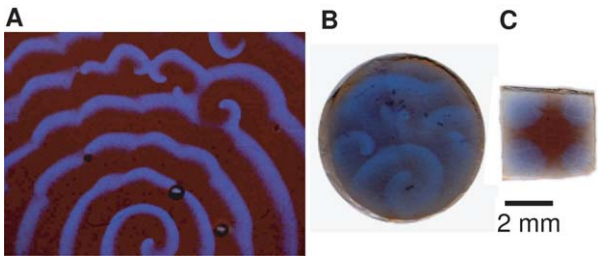

Fig. 1 BZ reaction with ferroin catalyst (A) in solution (B) in a 7.7 mm-diameter polyacrylamide-silica gel composite disc containing electrostatically bound ferroin (C) in a 3.6 × 3.6 mm square of the same polyacrylamide-silica BZ gel. See Methods for BZ reaction conditions.

Although the polyacrylamide-ferroin BZ system can be used to study pattern formation (see Fig. 2A), the gradual desorption of electrostatically bound ferroin from the gel during the BZ reaction limits repeatability of studies over long timescales. Thus, to preclude catalyst desorption while observing pattern formation within BZ gels for extended durations, it is advantageous to use a gel system in which the catalyst is covalently bound to the polymer backbone. For this reason, the poly(NIPAAm-*co*-$Ru(bpy)_3$) gel containing covalently bound ruthenium catalyst ($Ru(bpy)_3$) was synthesized according to established protocols.[12,26,27] In this BZ gel, the chemical waves are also visible: oxidation of the $Ru(bpy)_3$ catalyst (3^+ state) corresponds to a green hue and swollen gel network, whereas reduction (2^+ state) corresponds to an orange hue and contracted gel network.[9] We used this system to study quantitatively how size and shape affect pattern formation, by cutting rectangular gels of various mm-scale dimensions. Note that these gels provided high color contrast to characterize oscillation patterns, but were of relatively large lateral dimensions and relatively low $Ru(bpy)_3$ concentrations (5.4 mM); thus, concurrent changes in gel size *via* swelling were negligible. Gels were immersed in BZ reactants (malonic acid, sodium bromate, and nitric acid) to initiate the BZ reaction at time zero, and the oscillations were monitored *via* timelapse video microscopy at a constant solution temperature of 20 °C (see Methods). We considered three different aspect ratios, defined as the ratio of the rectangle length divided by width. Fig. 2 demonstrates that at early reaction times, pattern formation was sensitive to changes in aspect ratio. In particular, for an aspect ratio of 1, BZ waves penetrated from the corners of the square gel (Figs. 2A–B). For an aspect ratio of 2, these waves originated from either two points near each gel end or directly at the gel ends (Fig. 2C). Finally, for an aspect ratio of 3.7, the BZ reaction was more sensitive to fluctuations in the experimental

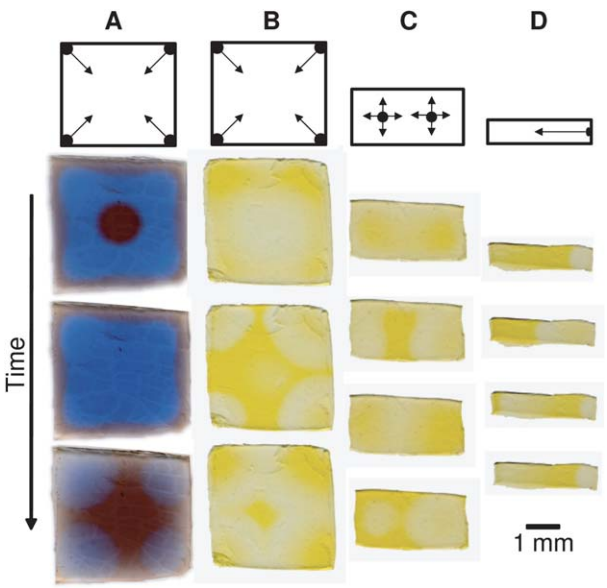

Fig. 2 BZ pattern formation at early reaction times. (A) 3.6 × 3.6 mm polyacrylamide-silica-ferroin composite; (B–D) poly(NIPAAm-*co*-$Ru(bpy)_3$) gels comprising 5.4 mM $Ru(bpy)_3$ catalyst and lateral dimensions of (B) 3.3 × 3.3 mm, (C) 3.1 × 1.6 mm, or (D) 3.0 × 0.8 mm. See Methods for BZ reaction conditions.

conditions (such as adhesion to the underlying Petri dish): waves initiated either from both ends of the gel and propagated inwards or from one end of the gel and travelled toward the opposite end (see Fig. 2D). The latter result resembles the unidirectional wave propagation reported by Yoshida *et al.* for narrow gel strips of aspect ratios up to approximately 20 and fixed at one end.[28–30] The induction time of visible oscillations varied insignificantly with gel aspect ratio, and the wave patterns initiated 1–3 min after gels were immersed in BZ reactants. Generally, Fig. 2 illustrates that as the corners of the gel and sites of BZ initiation are in closer spatial proximity, the global pattern transitions from initiation at gel corners to initiation at gel ends. This finding was repeatable for at least 4 replicate samples and experiments for each aspect ratio; Fig. 2 shows representative images. While it has been noted that gel thickness also influences pattern formation,[25] the results shown in Fig. 2 were consistent over a range of gel thickness (0.7 to 1.3 mm). Together, these results demonstrate that initial oscillation patterns within BZ gels can be modulated by changes in gel size and shape.

Indeed, shape-dependent pattern formation at early reaction times is anticipated from the nature of the BZ reaction confined within gels. Physically, the BZ reaction initiates only when the solution phase reactants diffuse into the gel to encounter the covalently bound metal catalyst. Initial concentration gradients within the gel vary according to aspect ratio, resulting in visibly different BZ pattern initiation. While transient patterns have also been recorded for BZ gels containing noncovalently bound ferroin catalyst, previous results[25] were observed in systems too large (>1 cm) for shape and size to influence BZ patterns. Further, those gel and reaction conditions produced highly irregular color oscillations, in contrast to the distinct and robust wave patterns shown in Fig. 2.

For each aspect ratio considered, the self-oscillating patterns changed appreciably after approximately 30 min. At longer reaction times (Fig. 3A), oscillation patterns became independent of aspect ratio: BZ waves consistently originated from the gel center and propagated radially toward the gel perimeter. These new patterns were recorded for over 2.5 h, at which point the experiments were terminated. These experimental results generally match those predicted from our BZ gel simulations at late reaction times (Fig. 3B): waves originate in the gel center and migrate radially outwards, regardless of aspect ratio. For the simulation images shown in Fig. 3B, blue and green correspond to a higher and lower concentration of oxidized catalyst, respectively, corresponding to those measured in our experiments. It is important to note that the behavior reported in Fig. 3B is highly robust: simulations for a wide range of system parameters and sample sizes/aspect ratios show that these late-time patterns propagate radially from the sample's center towards its edges.

The physical mechanism underlying pattern change at late reaction times is governed by the changing distribution of BZ reactants within the gel. There is a distinct difference between the inner and outer regions of the sample; namely, the exchange between reactants within the gel network and the external, bulk solution is more pronounced at the sample's boundaries. As a result, the gel center is the most likely point of wave initiation at late oscillation times, as is observed consistently in our experiments and simulations. Yamaguchi *et al.* have also observed

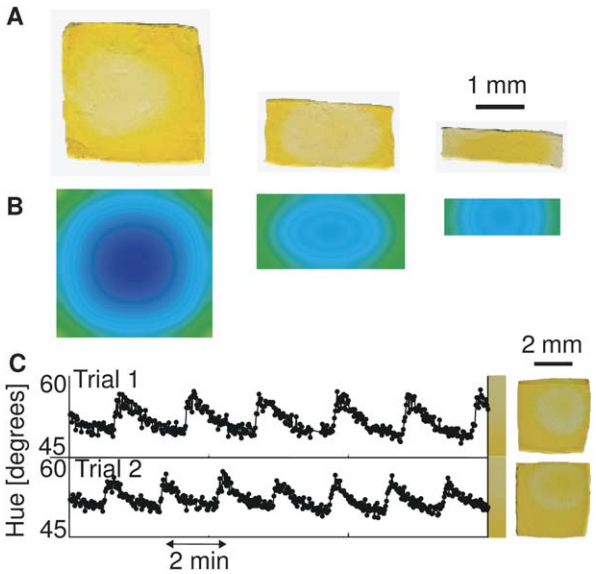

Fig. 3 BZ pattern formation at late reaction times. (A) poly(NIPAAm-*co*-Ru(bpy)$_3$) gels comprising 5.4 mM Ru(bpy)$_3$ catalyst and dimensions given in Fig. 2; (B) Simulation predictions for the same gel dimensions; (C) A single gel (3.7 × 3.7 mm) recycled in replicate trials. See Methods for BZ reaction conditions and Supplementary Information for simulation parameters.

temporal evolution of patterns in BZ gels containing ferroin catalyst, noting that patterns became more regular as the chemical concentrations within the gel became more uniform.[25] Further, we note that BZ reactions within a single-phase solution also have been reported to undergo a transient regime at the start of the reaction, characterized by inconsistent oscillations and patterns.[23,31,32] Thus, although the change in pattern formation at late reaction times is not unexpected, our results demonstrate the importance of documenting experimental results in such active soft matter over sufficiently long reaction times. Otherwise, it is difficult to distinguish between well-developed, robust oscillation behavior and transient patterns that are affected by initial conditions, including gel shape and size.

We note that we observed an inversion of this oscillating pattern at late reaction times for gels of aspect ratio 3.7 in Fig. 3A: these gels reproducibly exhibited waves of *reduced* catalyst originating from the center of the gel, whereas experiments for gels of lower aspect ratio exhibited waves of *oxidized* catalyst originating from the gel center. It is likely that this late-time redox pattern inversion is related to conditions under which absolute dimensions of the gel become comparable to diffusion length scales of the intermediate reaction species. It is worth noting that our simulations do not predict this pattern inversion at late reaction times for gels of aspect ratio 3.7. This is not surprising because we used a simplified model for the BZ reaction, which does not explicitly account for all intermediate reaction species.

To quantify the patterns formed at late reaction times, we determined the period of oscillation based on the waves of oxidized Ru(bpy)$_3$ catalyst, quantified according to hue at representative points within the gel and at least 30 min into the reaction (see Methods and ESI Fig. S1‡). Simulations predicted

a period of oscillation of approximately 2 min, varying insignificantly with gel aspect ratio (see ESI Fig. S4‡). Experiments showed that the period of oscillation was 2.1 ± 0.1 min for gels of aspect ratio 1 and 2, and was 11.1 ± 0.5 min for gels of aspect ratio 3.7. Thus, both the redox pattern inversion and oscillation period observed in gels of aspect ratio 3.7 deviate from simulation predictions. We attribute this discrepancy to the absolute dimensions of these gels, not the aspect ratio; see ESI Fig. S2‡ for oscillation period as a function of gel size.)

It is important to note that the reported late time patterns and periods of oscillation were consistent for both freshly prepared and recycled samples. In fact, Fig. 3C shows that the same gel sample can undergo the BZ reaction twice without change in pattern formation, duration of the reaction, or period of oscillation. In replicate trials, the reaction was monitored for >2.5 h and exhibited oscillation periods of 2.4 ± 0.2 min and 2.1 ± 0.6 min, respectively. This ability to reuse BZ gels is of particular note, given the highly acidic reaction conditions required to sustain self-oscillation.

Finally, we confirm quantitatively that synchronized chemomechanical coupling is observed for our gels when the BZ reaction is further confined within gels of sufficiently small dimensions, as noted extensively for this BZ gel type by Yoshida *et al.*[12] Aihara *et al.* estimated the critical length scale for this reaction to be ~0.6 mm in BZ resins, and showed that the mode of pattern formation changes below this critical size due to a switch in competition between kinetic and transport rates. In particular, traveling chemical waves give way to uniform oscillations in smaller systems.[33] For BZ gels, active mechanical swelling/shrinking is synchronized with chemical oscillations: the gel swells when the catalyst is homogeneously oxidized and shrinks when the catalyst is reduced.[9,12] Figs. 4A–B demonstrate this chemomechanical behavior for a gel of ~0.6 mm edge lengths and 8.3 mM $Ru(bpy)_3$ concentration, exhibiting oscillations every 21.2 ± 2.5 min and lasting >3.5 h. This chemically-induced swelling corresponded to a maximum change in the projected area of the triangular gel of 14.2 ± 2.1%, or a volumetric swelling of 21.9 ± 3.4%.

The amplitude of gel swelling also increases with increasing $Ru(bpy)_3$ catalyst content, which scales with the color saturation of the gel (Fig. 4C). Experiments for gels of edge lengths <0.6 mm demonstrate this quantitatively, and are consistent with our paired simulations for gels of similar dimensions and range of $Ru(bpy)_3$ concentration. Further, the period of oscillation depends both on $Ru(bpy)_3$ content and on physical size (Fig. 4D). This size-dependence of oscillation period has also been noted by Yoshida *et al.* and Yamaguchi *et al.*, who attributed increased oscillation periods to decreased transport rates in very small or thin gels.[12,25] The present experiments show that for a given $Ru(bpy)_3$ concentration, the period of oscillation can increase as much as threefold for samples of dimensions smaller than the critical length scale. This finding cannot be reproduced by our simulations. Fig. 4D indicates that there is a discrepancy between simulation predictions and experimental results for gels characterized by lateral dimensions <0.6 mm. Interestingly, the gel of aspect ratio 3.7 in Figs. 2D and 3A (which produced oscillation periods and late-time patterns in contrast to simulations) exhibits a width of 0.8 mm that shrinks to 0.5 mm in the acidic conditions of the BZ reaction. As noted previously, the

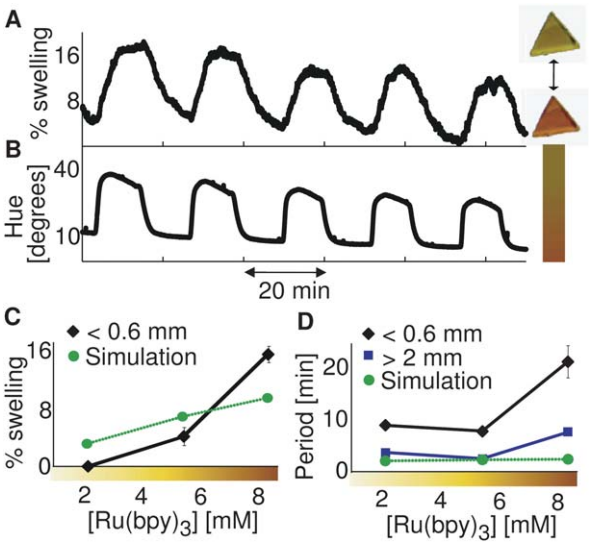

Fig. 4 Synchronized chemical and mechanical oscillations in poly(-NIPAAm-*co*-$Ru(bpy)_3$) gel of 0.6 mm edge lengths. (A) Swelling and shrinking of the gel are coupled to (B) oscillating change in oxidation state of the $Ru(bpy)_3$ catalyst (8.3 mM), confirming the expected coupling for successfully polymerized BZ gels of sufficiently small dimensions. (C) % swelling of the projected gel area; and (D) oscillation period as a function of $Ru(bpy)_3$ catalyst concentration within the gel. Legend indicates approximate lateral dimensions for each gel. Error bars represent standard deviation. See Methods for BZ reaction conditions and catalyst concentration measurements, and Supplemental Information for simulation details.

reaction model of our simulations does not account for all intermediate reaction species, and this simplification may introduce deviations from experiments for gels of edge lengths below this critical length scale. Both our experiments and simulations show that the period depends only mildly on $Ru(bpy)_3$ concentration when gel dimensions exceed this critical length scale. We note that the increase in oscillation period with increasing $Ru(bpy)_3$ content exists but is significantly smaller in simulations than in experiments, as discussed in Supplementary Information. We emphasize that through a direct comparison between experiments and simulation, we were able to estimate the strength of the chemomechanical coupling in the BZ gels. In particular, we could extract a realistic value for our model parameter χ^* (see ESI‡), which relates the mechanical response of the gel to the degree of oxidation of the catalyst.

Conclusions

In summary, this study elucidates how confinement of the BZ reaction within millimetre-sized gels modulates pattern formation and chemomechanical swelling. Experimental demonstration of shape- and size-dependent pattern initiation and evolution provides context for previously reported behavior in such self-oscillating gels. Our results show that at early reaction times, pattern formation depends on gel size, shape, and perturbation of initial conditions. At late reaction times, however, pattern formation becomes independent of gel dimensions. Direct comparison between these experiments and simulations provides a validation of our theoretical and numerical

models of chemomechanical coupling in these complex, active materials. Moreover, utilizing an improved model for the reaction kinetics, our simulations allow us to account for the effects of the total concentration of the grafted catalyst on the dynamics of such active gels, and to identify length scales at which a more detailed reaction kinetics model should be employed. These findings can thus ground future studies that leverage the strong coupling between chemical and mechanical states within these active hydrogels, enabling new applications and biological analogues that exhibit self-oscillation.

Methods

Synthesis of poly(NIPAAm-*co*-Ru(bpy)$_3$)

The monomer catalyst, ruthenium(4-vinyl-4-methyl-2,2-bipyridine)bis(2,2-bipyridine)bis(hexafluorophosphate) (Ru(bpy)$_3$) was synthesized from commercially available 4,4′-Dimethyl-2,2′-bipyridine and Ru(bpy)$_2$Cl$_2$.[26,27] NIPAAm monomer (160 mg), Ru(bpy)$_3$ monomer (2–9 mg), N,N′-methylenebisacrylamide (MBAAm) (2.8 mg) crosslinker, and 2,2-azobis(isobutyronitrile) (AIBN) (6.6 mg) initiator were dissolved in methanol (1 mL) and degassed with nitrogen for 4 min. The solution was polymerized in a vial for 18 h at 60 °C. The resulting gel was soaked in methanol for 1 week to remove unreacted monomers and gradually hydrated.[28] To determine catalyst concentration within the gel, absorption at $\lambda = 457$ nm was measured *via* UV/Vis spectrophotometry to quantify unreacted Ru(bpy)$_3$ monomer. The approximate yield of polymerized Ru(bpy)$_3$ monomer ranged between 77–91%. All reagents were obtained from Sigma-Aldrich, except for the Ru(bpy)$_2$Cl$_2$ obtained from Acros Organics.

Synthesis of polyacrylamide-silica gel containing ferroin

Solutions comprising 40% acrylamide (2.5 mL), N,N′-methylenebisacrylamide (MBAAm) (15.2 mg), TEMED (51.7 μL), AMPS (79.2 mg), and sodium silicate (800 μL of 10.6% Na_2O, 26.5% SiO_2 solution) were dissolved in water (7.5 mL) and 1 mL volumes were allowed to polymerize for one day. The resulting gel was soaked in water for 3 days, and soaked in ferroin (12 mM) for 15 days. The gel was washed with water to remove unbound ferroin.[10] All reagents were obtained from Sigma-Aldrich.

Initiation and imaging of BZ reaction

The BZ solution was prepared using either ferroin (5 mM), sulfuric acid (0.3 M), malonic acid (0.2 M), and sodium bromate (0.3 M) for the reaction in solution; or sulfuric acid (0.6 M), malonic acid (60 mM), and sodium bromate (80 mM) for the polyacrylamide system;[10] or nitric acid (0.9 M), malonic acid (63 mM), and sodium bromate (84 mM) for the poly(NIPAAm-*co*-Ru(bpy)$_3$) system.[8] Before adding the BZ reactants to the gel, the solution was degassed with nitrogen and sonicated under vacuum. To prepare the BZ gel sample, storage water was aspirated from the gel. The sample remained hydrated but the surrounding petri dish did not contain excess water. To initiate the BZ reaction, 5 mL of filtered BZ solution was pipetted directly on top of the gel such that the gel was well-submerged in an unstirred, BZ solution. Time-lapse imaging at room temperature was recorded for 2–4 h under a stereomicroscope (Olympus, SZX7) with an LED light and camera (Olympus, DP25).

Characterization of BZ reaction in gels

Images of the gel were analyzed *via* ImageJ to quantify hue as defined with cylindrical coordinates on the RGB color space.[34] Patterned gels lacking homogenous color change were analyzed at representative points of interest to extract period and wave velocity. See Supplementary Information for detailed calculations of hue and wave velocity. Small gels exhibiting homogenous color change were analyzed by averaging hue over the entire projected area of the gel at each frame. To calculate the degree of swelling in small gels, the dynamic projected area was determined using ImageJ. To compare the degree of swelling and period for gels containing varying Ru(bpy)$_3$ concentrations, the first five oscillations in each gel were quantified and presented as average ± standard deviation. For small gels, the period was consistent throughout the reaction duration.

Simulation of BZ reaction in gels

Simulations were conducted by using a three-dimensional gel lattice spring model (3D gLSM) approach as described previously.[15] Here, however, we modified the reaction kinetics scheme we employed in our original approach[13,15,21] by incorporating an improved Oregonator model,which explicitly includes the concentration of Ru(bpy)$_3$ in the governing equations.[22] This modified approach allowed us to model for the first time the effect of the total concentration of Ru(bpy)$_3$ on the period of oscillations, amplitude in the degree of swelling, as well as pattern formation in the three-dimensional BZ gel samples. Importantly, this modified approach also allowed us to demonstrate that our original modeling of the BZ reaction kinetics in chemo-responsive gels[13,15,21] is applicable if the concentration of Ru(bpy)$_3$ is sufficiently high (see Supplementary Information for more details). Here, we adjusted our simulation parameters to match experimental conditions and used the specific gel dimensions and catalyst concentrations employed in the experiments. Details of the modified equations for the reaction kinetics in gLSM, the simulation parameter values, as well as detailed discussion of the dependence of the period of oscillations for all sample sizes on the dimensionless total concentration of Ru(bpy)$_3$ catalyst are provided in the ESI.‡

Acknowledgements

We acknowledge the Institute for Soldier Nanotechnology at MIT for facility access. ACB also acknowledges partial support from ARO (for VVY). This work was supported primarily by the MRSEC Program of the National Science Foundation under award number DMR-0819762.

References

1 M. K. Beyer and H. Clausen-Schaumann, *et al.*, *Chem. Rev.*, 2005, **105**(8), 2921–2948.
2 D. Kuckling, *Colloid Polym. Sci.*, 2009, **287**(8), 881–891.

3 T. Miyata, K. Nakamae, A. S. Hoffman and Y. Kanzaki, *Macromol. Chem. Phys.*, 1994, **195**(4), 1111–1120.
4 T. Tanaka, I. Nishio, S. Sun and S. Ueno-Nishio, *Science*, 1982, **218**, 467–469.
5 T. Miyata, T. Uragami and K. Nakamae, *Adv. Drug Delivery Rev.*, 2002, **54**(1), 79–98.
6 Y. Osada, H. Okuzaki and H. Hori, *Nature*, 1992, **355**(6357), 242–244.
7 D. J. Schmidt, F. C. Cebeci, Z. I. Kalcioglu, S. G. Wyman, C. Ortiz, K. J. Van Vliet and P. T. Hammond, *ACS Nano*, 2009, **3**(8), 2207–2216.
8 R. Yoshida, S. Onodera, T. Yamaguchi and E. Kokufuta, *J. Phys. Chem. A*, 1999, **103**(43), 8573–8578.
9 R. Yoshida, *Adv. Mater.*, 2010, **22**, 3463–3483.
10 I. Y. Konotop, I. R. Nasimova, N. G. Rambidi and A. R. Khokhlov, *Polym. Sci., Ser. B*, 2009, **51**(9–10), 383–388.
11 H. Degn, *J. Chem. Educ.*, 1972, **49**(5), 302–307.
12 R. Yoshida, M. Tanaka, S. Onodera, T. Yamaguchi and E. Kokufuta, *J. Phys. Chem. A*, 2000, **104**(32), 7549–7555.
13 V. V. Yashin and A. C. Balazs, *Macromolecules*, 2006, **39**(6), 2024–2026.
14 V. V. Yashin and A. C. Balazs, *Science*, 2006, **314**(5800), 798–801.
15 O. Kuksenok, V. V. Yashin and A. C. Balazs, *Phys. Rev. E: Stat., Nonlinear, Soft Matter Phys.*, 2008, **78**(4), 041406.
16 V. V. Yashin, O. Kuksenok and A. C. Balazs, *Prog. Polym. Sci.*, 2010, **35**(1–2), 155–173.
17 O. Kuksenok, V. V. Yashin, P. Dayal, and A. C. Balazs, Self-Oscillating Gels as Biomimetic Soft Materials in *Nonlinear Dynamics with Polymers: Fundamentals, Methods and Applications*, ed. J. A. Pojman, Q. Tran-Cong-Miyata, John Wiley & Sons, 2010, pp. 135–162.
18 O. Kuksenok, V. V. Yashin and A. C. Balazs, *Soft Matter*, 2007, **3**(9), 1138–1144.
19 O. Kuksenok, V. V. Yashin and A. C. Balazs, *Soft Matter*, 2009, **5**(9), 1835–1839.
20 V. V. Yashin, K. J. Van Vliet and A. C. Balazs, *Phys. Rev. E: Stat., Nonlinear, Soft Matter Phys.*, 2009, **79**(4), 46214.
21 V. V. Yashin and A. C. Balazs, *J. Chem. Phys.*, 2007, **126**(12), 124707.
22 T. Amemiya, T. Yamamoto, T. Ohmori and T. Yamaguchi, *J. Phys. Chem. A*, 2002, **106**(4), 612–620.
23 I. R. Epstein and K. Showalter, *J. Phys. Chem.*, 1996, **100**(31), 13132–13147.
24 A. S. Mikhailov and K. Showalter, *Phys. Rep.*, 2006, **425**(2–3), 79–194.
25 T. Yamaguchi, L. Kuhnert, Z. Nagy-Ungvarai, S. C. Mueller and B. Hess, *J. Phys. Chem.*, 1991, **95**(15), 5831–5837.
26 P. Ghosh and T. G. Spiro, *J. Am. Chem. Soc.*, 1980, **102**(17), 5543–5549.
27 X. Schultze, J. Serin, A. Adronov and J. M. J. Fréchet, *Chem. Commun.*, 2001, (13), 1160–1161.
28 S. Maeda, Y. Hara, T. Sakai, R. Yoshida and S. Hashimoto, *Adv. Mater.*, 2007, **19**(21), 3480–3484.
29 Y. Murase, S. Maeda, S. Hashimoto and R. Yoshida, *Langmuir*, 2009, **25**(1), 483–489.
30 R. Yoshida, E. Kokufuta and T. Yamaguchi, *Chaos*, 1999, **9**(2), 260–266.
31 M. Rustici, M. Branca, C. Caravati and N. Marchettini, *Chem. Phys. Lett.*, 1996, **263**(3–4), 429–434.
32 M. Rustici, C. Caravati, E. Petretto, M. Branca and N. Marchettini, *J. Phys. Chem. A*, 1999, **103**(33), 6564–6570.
33 R. Aihara and K. Yoshikawa, *J. Phys. Chem. A*, 2001, **105**(37), 8445–8448.
34 A. Hanbury, *Pattern Recognit. Lett.*, 2008, **29**(4), 494–500.